Solvatochromism of BODIPY–Schiff dye

6 AUTHORS, INCLUDING:

Aleksander Filarowski
University of Wroclaw
76 PUBLICATIONS   1,240 CITATIONS

SEE PROFILE

Mark Van der Auweraer
University of Leuven
333 PUBLICATIONS   8,467 CITATIONS

SEE PROFILE

Wim Dehaen
University of Leuven
568 PUBLICATIONS   9,277 CITATIONS

SEE PROFILE

Solvatochromism of BODIPY-Schiff Dye

Aleksander Filarowski,[*,†,‖] Marina Lopatkova,[†] Paweł Lipkowski,[‡] Mark Van der Auweraer,[§] Volker Leen,[§] and Wim Dehaen[§]

[†]Faculty of Chemistry, University of Wroclaw, F. Joliot-Curie 14, 50-383 Wrocław, Poland

[‡]Theoretical Chemistry Group, Institute of Physical and Theoretical Chemistry, Wrocław University of Technology, Wyb. Wyspiańskiego 27, 50-370 Wrocław, Poland

[§]Department of Chemistry, Katholieke Universiteit Leuven, Celestijnenlaan 200f−bus 02404, 3001 Leuven, Belgium

[‖]Tyumen State University of Architecture and Civil Engineering, 625001 Tyumen, Russia

Ⓢ *Supporting Information*

ABSTRACT: A boron−dipyrrin chromophore connected with an *o*-hydroxyaryl aldimine by a diazo bridge (BODIPY-Schiff dye) has been developed. The photophysical properties of the BODIPY-Schiff dye have been investigated with UV, steady-state, and time-resolved fluorimetry. The spectral features have been characterized with respect to density functional theory and time-dependent density functional theory. The conformational analysis of the studied compound has been accomplished both in the ground and excited states. A scheme of the processes occurring in the BODIPY-Schiff dye has been proposed.
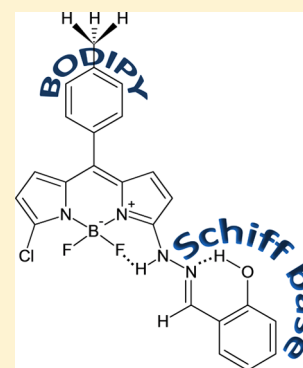
■ INTRODUCTION

Presented investigations deal with a chromophore which is intensively studied nowadays.[1−3] The system synthesized and analyzed in this work is a combination of a strong chromophore (4,4′-difluoro-4-bora-3a,4a-diaza-*s*-indacene, BODIPY)[4−9] and an *o*-hydroxyaryl Schiff base (Scheme 1) which includes an intramolecular hydrogen bond and is characterized by photothermochromism.[10] The influence of both intramolecular hydrogen bonding and the tautomeric equilibrium on the spectral characteristics in the ground[11,12] and excited states[13−15] are properly described for *o*-hydroxyaryl Schiff bases. However, very few works study the influence of hydrogen bonding and a tautomeric equilibrium on BODIPY dyes.[16−19] This fact is of no surprise because hydrogen bonding decreases the fluorescence quantum yield,[20] so most works did not focus on this aspect. Ziessel et al.[16] performed the synthesis and spectral study of the combination of a 4,4′-difluoro-4-bora-3a,4a-diaza-*s*-indacene's core and a 6,6′-dimethyl-2,2′-bipyridine which is characterized by two OH···N hydrogen bonds. Surprisingly, the observed significant Stokes shift for 6,6′-dimethyl-2,2′-bipyridine,[21] conditioned by the proton transfer,[22] has not been traced for the combined compound. A similar situation was observed for BODIPY-benzoxazoles.[23] Reference 17 reveals that the direct influence of intramolecular hydrogen bonding on the 4,4′-difluoro-4-bora-3a,4a-diaza-*s*-indacene core provokes a red-shifted emission profile. To explain this phenomenon, the rigidification of 4,4′-difluoro-4-bora-3a,4a-diaza-*s*-indacene's core by means of BF···HN

intramolecular hydrogen bonding was assumed. It is important to note the positive role of intramolecular hydrogen bonding to solve the "concentration quenching" problem. So, the complex of 1,2-bis[2-methyl-5-(4-pyridil)-3-thienyl]cyclopentene (pyridyl derivative) with two *meso*-carboxyphenyl BODIPYs is characterized by a 10-fold increase of the fluorescence intensity and a blue shift of the absorption band ($S_0−S_1$) by 65 nm due to the intermolecular hydrogen bond formation in the solution.[18] The opposite trend is observed for the *meso*-pyridine derivative of BODIPY.[24] Upon protonation of the pyridine fragment a large shift of the absorption band is observed while the emission band showed no shift. However, a significant quenching of the fluorescence was observed.[24] Similar spectral changes were observed for the complex of 3-indole-BODIPY's derivative with a fluoride anion.[25]

One of the pioneer investigations on the influence of a keto−enol tautomerism on the spectral characteristics of BODIPY has been published in ref 26. According to this investigation, the -CH=C(C₆H₅)−OH ⇌ -CH₂−C(C₆H₅)=O tautomeric equilibrium in BODIPY induces a significant bathochromic shift of the absorption band upon increasing the solvent polarity. This confirmation is in agreement with the studies of

Scheme 1. Chemical Structure of Combination BODIPY Dye and *o*-Hydroxyaryl Schiff Base and a Scheme of the Isomerization and Tautomeric Equilibrium in Schiff Fragment
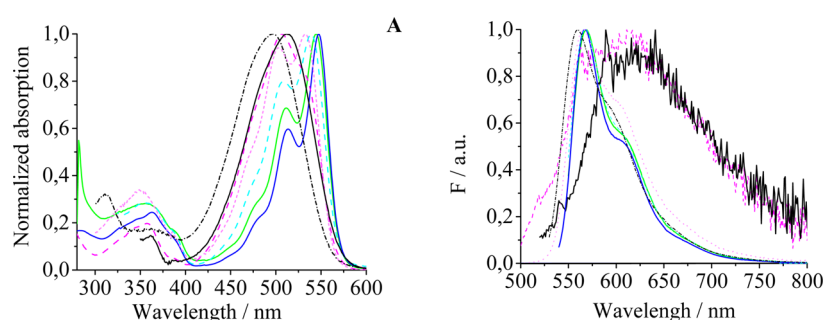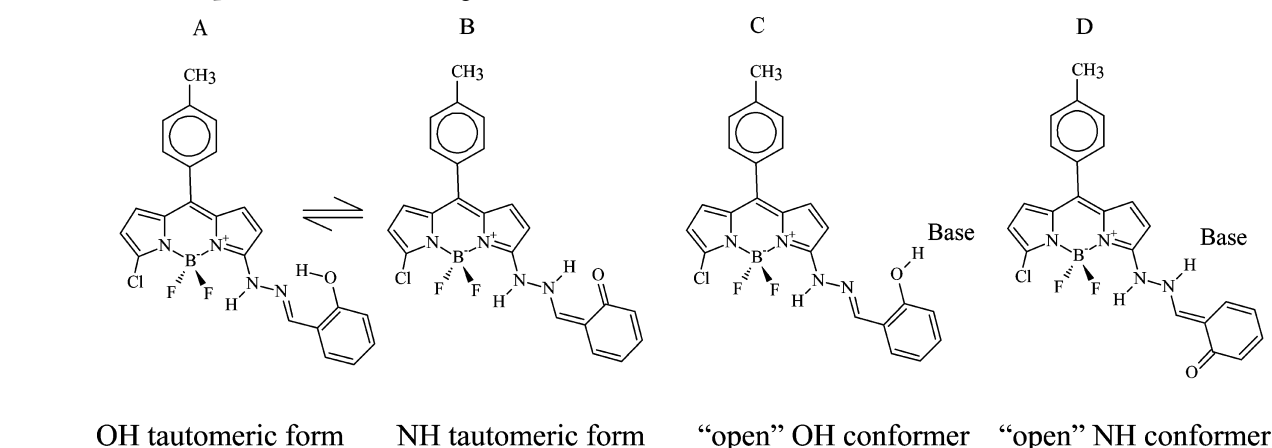

OH tautomeric form   NH tautomeric form   "open" OH conformer   "open" NH conformer

Figure 1. Selected absorption (A) and emission (B) spectra of BODIPY-Schiff dye in different solvents normalized to 1.0. Ethanol + TFA (black, short dashed−dotted line), ethanol + KOH (magenta, dashed line), DMFA (black, solid line), 1-butanol (light magenta, short dashed line), 1,2-dichloroethane (cyan, dashed line), toluene (green, solid line), CCl$_4$ (blue, solid line).

the keto−enol tautomeric equilibrium.[27] The work by Ziessel et al.[19] presents the synthesis of pentane-2,4-dione BODIPY with an extremely strong hydrogen bridge (d(O−O) = 2.409(7) Å). Of great importance is the participation of protonation and deprotonation of the particular fragments of the BODIPY's dyes[8,9,23,28−31] in the design of the fluorescence switches. In the works discussed previously the effects of intermolecular hydrogen bonding type[16,17,19] as well as the direct impact of BF···HN intramolecular hydrogen bonding on BODIPY's dyes[18] are presented. This work dwells particularly on the influence of an *o*-hydroxyaryl aldimine moiety in position 3 of BODIPY's chromophore (Scheme 1). For the *o*-hydroxyaryl aldimine fragment one has to consider at least the following two processes: the -OH···N $\rightleftarrows$ O$^-$···HN$^+$ tautomeric equilibrium and cis−trans isomerization. On the one hand, intramolecular hydrogen bonding is supposed to decrease the fluorescence quantum yield while, on the other hand, the proton-transfer process and the formation of a zwitterionic form (as well as the process of trans−cis isomerization) are expected to induce a visible Stokes shift and to influence the charge transfer between the *o*-hydroxyaryl aldimine and the 4,4′-difluoro-4-bora-3*a*,4*a*-diaza-*s*-indacene's core.

■ EXPERIMENT AND CALCULATIONS

All solvents used for the spectroscopic measurements were of spectroscopic grade and were used as received. The chemicals for the synthesis were of reagent grade quality, procured from commercial sources. Boron trifluoride etherate, ca. 48% BF$_3$, was from Acros Organics. The starting compound 4,4-difluoro-8-[4-(methyl)phenyl]-1,3-dichloro-3*a*,4*a*-diaza-4-bora-*s*-indacene was synthesized according to the published procedure.[32] The fluorescent BODIPY-Schiff dye was obtained via condensation of 4,4-difluoro-8-[4-(methyl)phenyl]-1,3-dichloro-3*a*,4*a*-diaza-4-bora-*s*-indacene with salicylaldehyde hydrazone (Acros) without catalyst.[33] A scheme of synthesis is presented in the Supporting Information (Scheme S1).

Dilute solutions of the BODIPY-Schiff dye in different solvents were prepared by dissolving the dry, powdered dye in the appropriate solvent so that the absorbance at the maximum of the main absorption peak was ≤0.1. Freshly prepared samples in 1 cm quartz cells were utilized to perform all measurements. UV−vis absorption spectra (Figure S1 of the Supporting Information) were recorded on a PerkinElmer Lambda 40 UV−vis spectrophotometer. Selected spectra are presented in Figure 1A. For the corrected steady-state excitation and emission spectra, a SPEX Fluorolog was used. Cresyl violet in methanol (Φ_f = 0.55) was used as fluorescence standard for the quantum yield (Φ_f) determinations.[34] In all cases, the correction for the solvent refractive index was applied. The relative error on Φ_f amounts to less than 10%. The fluorescence spectra and quantum yields were performed at 20 °C using undegassed samples. The fluorescence decays of the BODIPY-Schiff dye were recorded at several emission wavelengths using the single-photon timing method.[35] Details of the experimental procedures have been described earlier.[36] The standard errors of all fluorescence lifetimes τ are ≤10 ps. The Φ_f and τ values in the used solvents are reported in Tables 1 and 2.

2577

dx.doi.org/10.1021/jp508718d | J. Phys. Chem. B 2015, 119, 2576−2584

Table 1. Spectroscopic/Photophysical Data of BODIPY-Schiff Dye in Different Solvents

	solvent	ε	$\lambda_{abs,1}$ (max/nm)	$\lambda_{abs,2}$ (max/nm)	λ_{em} (max/nm)	$\Delta\bar{\nu}^a$ (cm^{-1})	Φ_f
1	cyclohexane	2.0	545	512	564	596	0.249
2	1,4-dioxane	2.2	537	506	567	985	0.343
3	toluene	2.4	545	512	568	755	0.257
4	CCl$_4$	2.4	547	513	568	676	0.396
5	isopropyl ether	3.9	538	506	563	812	0.165
6	dibutyl ether	3.1	541	508	564	754	0.186
7	diethyl ether	4.3	536	504	561	845	0.125
8	chloroform	4.8	543	510	570	857	0.166
9	ethyl acetate	6.0	530	503	565	1179	0.115
10	THF	7.5	534	506	568	1136	0.112
11	1-undecanol	8.1	541	509	570	940	0.295
12	trifluoroethanol	8.6	526	497	560	1148	0.138
13	1-octanol	10.3	535	507	568	1070	0.134
14	1.2-dichloroethane	10.7	539	508	567	920	0.222
15	1-pentanol	13.9	537	507	567	997	0.129
16	1-butanol	17.8	506		564	2171	0.044
17	2-propanol	18.3	505		564	2056	0.022
18	acetone	20.7	509		565	1928	0.003
19	ethanol	24.5	504		566	2194	0.035
20	ethanol + TFA^b		532	504	566	2180	0.087
21	ethanol + HCl(1N)^b		533	503	566	2184	0.085
22	ethanol + KOH(1N)^b		499		615	3780	0.000
23	methanol	33.1	501		564	2203	0.021
24	DMF	36.7	512		624	3506	0.000
25	acetonitrile	37.5	523	501	573	2508	0.001
26	acetonitrile + N(Et)$_3$(5%)		509		610	3252	0.000
27	DMSO	46.7	513		627	3506	0.000

$^a\Delta\bar{\nu}$, Stokes shift. ^{b}One drop of TFA, HCl(1N), and KOH(1N) was added to solutions 20, 21, and 22 of ethanol, respectively.

Table 2. Lifetime (τ, ns) of BODIPY-Schiff Dye in Different Solvents

	solvent	τ	
1	cyclohexane	1.832	
2	1,4-dioxane	1.916	
3	toluene	2.148	
4	carbon tetrachloride	2.510	
5	isopropyl ether	1.568	
6	dibutyl ether	1.978	
7	diethyl ether	1.402	
8	chloroform	2.447	
9	ethyl acetate	1.457	
10	THF	1.349	
11	1-undecanol	2.596	
13	1-octanol	2.244	
14	1.2-dichloroethane	2.100	
15	1-pentanol	1.363	1.957
16	1-butanol	1.331	2.297
17	2-propanol	0.687	1.448
18	acetone	0.299	0.939
23	methanol	0.224	0.775

The calculations were performed using the Gaussian 09 program[37] with a 6-31+G(d,p) basis set[38−40] and the hybrid Hartree−Fock density functionals (B3LYP[41−43] and PBE0[44]). The use of diffuse functions was necessary to study the hydrogen bonding.[45] The quantum-mechanical calculations were employed for the ground (density functional theory, DFT[46]) and excited (time-dependent density functional theory, TD-DFT[47,48]) states for gas phase and the set of solvents. The influence of solvent effects was taken into account the using polarizable continuum model (PCM)[49] and the linear-response (LR) approach[50] as default.

RESULTS AND DISCUSSION

Analyses of Spectroscopic Dependencies. In solvents of low and medium polarity (from cyclohexane to tetrahydrofuran (THF)) the absorption maximum is situated between 534 and 547 nm while a second maximum, which can be attributed to vibrational progression (1200 ± 20 cm^{-1}), is observed between 504 and 513 nm. The small blue shift parallels a decrease of solvent polaris ability and an increase in solvent dipolar polarity. For this range of solvents the fluorescence spectra consist of a relatively narrow maximum and a shoulder red-shifted by about 30 nm. It is more difficult to find for this solvent range a trend in the fluorescence maximum. The increase of the Stokes shift upon increasing solvent polarity clearly suggests an increase of the dipole moment upon excitation. For this range of solvents the Stokes shift can be fitted to a Lippert−Mataga relationship (Figure 2). One should note that while the increase in Stokes shift is much smaller than in BODIPYs with an azacrown ether substituent (strong donor), it is larger than for BODIPYs with methyl or phenol substituent (weak donor) (Figure 2).[51,52] It is no surprise that the hydrazone nitrogen is a less outspoken donor than that of an aza crown ether as it is connected to the second electronegative nitrogen of the hydrazon. In this solvent range the fluorescence decay of the BODIPY dyes can be analyzed as an exponential curve. Upon increasing the solvent polarity both the fluorescent quantum yield (Table 1) and fluorescence decay
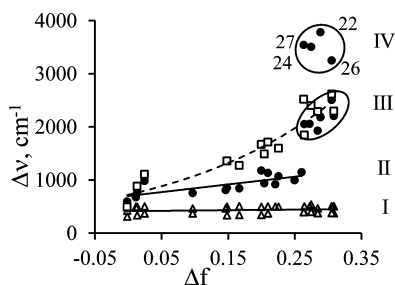
Figure 2. Stokes shift ($\Delta\bar{v}$) versus the Lippert solvent parameter ($\Delta f = f(\varepsilon) - f(n^2)$) plot for studied BODIPY-Schiff dye (black filled circles) and aza phenyl ether (open squares),[28] phenol,[51] methyl,[51] and imidazole[52] (open triangles) BODIPY's derivatives. The numbers refer to the solvents in Table 1.

Figure 3. Stokes shift ($\Delta\nu$) of studied BODIPY-Schiff dye as a function of the solvent polarity parameter $E_T^N(30)$. The numbers refer to the solvents in Table 1. The straight lines are the linear fits for the solvents with $\varepsilon < 17.8$ (II), $\varepsilon > 17.8$ (III), and DMSO, DMF, and C_2H_5OH + KOH (IV).

time (Table 2) decrease. However, the fluorescence quantum yield decreases twice as fast as the fluorescent decay time.

According to the obtained Lippert–Mataga dependence (Figure 2) one can confirm that the studied BODIPY-Schiff dye faces at least two significant changes under the transfer from the ground state to the exited state. Correlation I (Figure 2) reveals a kind of linear increase of Stokes shift under the growth of the Lippert parameter. A collation of this correlation (I) with those obtained earlier for phenol, imidazole, and methyl BODIPY's derivatives[51,52] makes it possible to assume that the BODIPY-Schiff dye brings about the growth of the molecule polarization under the increase of solvent polarity ($\varepsilon < 17.8$). The strengthening of the OHN intramolecular hydrogen bond is this phenomenon. A much stronger increase of the solvent polarity ($\varepsilon \geq 17.8$, curve II in Figure 2) evokes the intramolecular proton transfer in the excited state (ESPT) [enol-imine (ground state) → keto-amine (excited state)] (Scheme 1). This effect forces a larger Stokes shift (~2000 cm^{-1}) and hypsochromic shift of absorption band (Figures 1 and S1 (Supporting Information)). Such negative solvatochromism is explained as the electron-donor imine group (-C=N-) comes to be electron-acceptor under ESPT (protonation of imino group, -C=NH$^+$), which results in the hypsochromic shift according to the earlier results for the BODIPY derivatives.[30,53] However, this shift is atypical for the $\pi-\pi*$ absorption shift band of Schiff bases,[11] which is characterized by the bathochromic shift and the intramolecular proton transfer. The obtained points (II, Figure 2) are well correlated with those obtained earlier for the aza-crown-ether BODIPY's derivative[28] where visible changes of 15-crown-5-ether fragment are seen under the excited state.

Far more significant changes of the spectral values are traced for dimethyl sulfoxide (DMSO), dimethylformamide (DMF), C_2H_5OH + KOH, and CH_3CN + N(Et)$_3$ solutions. Such changes can be explained by the disruption of the intramolecular hydrogen bonding and the formation of the either intermolecular hydrogen bond ("open" conformers) with the possibility of cis−trans isomerization in the DMSO and DMF solutions or deprotonation of the Schiff base moiety (O$^-$N$^-$ ion in the C_2H_5OH + KOH and CH_3CN + N(Et)$_3$ solutions). In this case the electron-donor properties of the Schiff fragment are much strengthened; then the Stokes shift is much stronger (~3500 cm^{-1}, Table 1).

Visible changes are also observed for the $\Delta\bar{v} = f(E_T^N(30))$ dependence (Figure 3). This dependence analysis gives a good possibility to show a major difference in the interactions between protic solvent−BODIPY-Schiff dye and protic
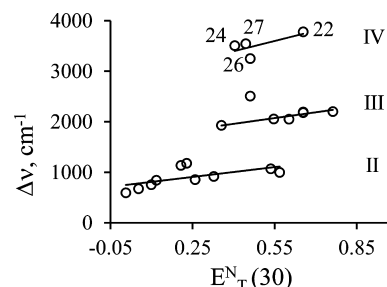
solvent−dimethylaminostyryl,[26,51] phenol,[51] and aza-phenyl-ether[28] BODIPY's derivatives. For dimethylaminostyryl, phenol, and aza-phenyl-ether BODIPY's derivatives, protic solvent decreases the Stokes shift due to the formation of the intermolecular hydrogen bonding which "switches off" (under protonation) the process of the charge transfer between the amine fragment and BODIPY's core, which then corresponds to the decrease of the Stokes shift. As for the BODIPY-Schiff dye studied in polar solvents ($\varepsilon \geq 17.8$) the intramolecular ESPT and the formation of the zwitterionic form are observed which intensify the polarization of the molecule and, consequently, the increase of the charge transfer between the Schiff moiety and BODIPY's core. This effect is related to the growth of the Stokes shift (correlation III, Figure 3). The aforesaid statement can be verified by the skip-like decrease of Φ_f on the border of $\varepsilon \geq 17.8$ from 0.13 to 0.04 unit (Table 1).

To summarize the analysis accomplished before, one can conclude that dimethylaminostyryl,[26,51] phenol,[51] and aza-phenyl-ether[28] BODIPY's fragments in the ground and excited states are either electron-donor or neutral substituents, whereas the studied Schiff fragment is electron-donor in the ground state and electron-acceptor in the excited state in the case of ESPT and zwitterion (curve III, Figure 3) or deprotonation of the Schiff base moiety (curve IV, Figure 3). Moreover, the presented dependencies $\Delta\nu = f(\Delta f)$ and $\Delta\bar{v} = f(E_T^N(30))$ allow one to predict some possible phenomena which occur in the molecule, but dependence $\Delta\lambda_{abs}, \Delta\lambda_{em} = f(\Delta f)$ (Figure 4) does not provide complete information.

Molecular Modeling of Processes in BODIPY-Schiff Dye. With the aim of defining a more stable conformer and prospective photochemical processes in the molecule, the
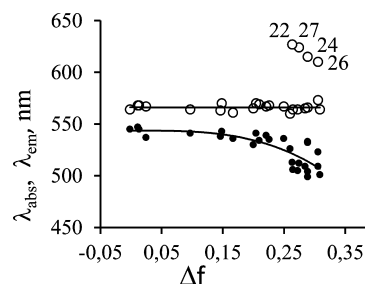

Figure 4. Maxima of the absorption (λ_{abs}, black filled points) and fluorescence emission (λ_{em}, open points) as a function of the Lippert solvent parameter (Δf) for the studied BODIPY-Schiff dye. The numbers refer to the solvents in Table 1.
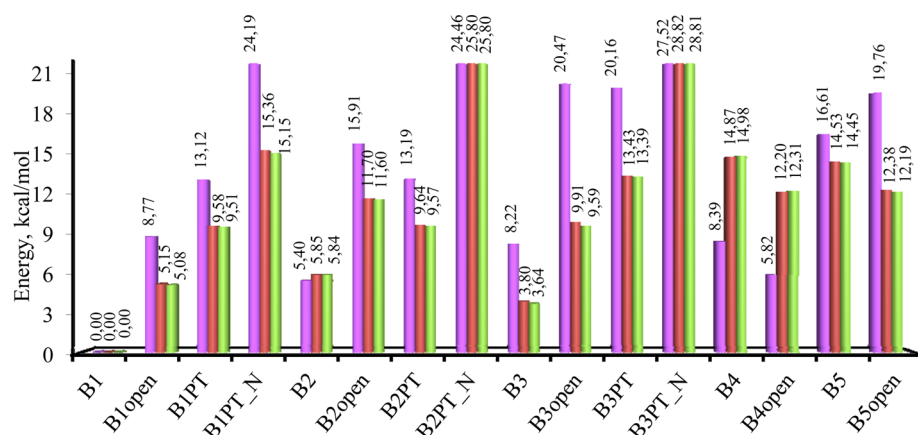
Figure 5. Energy difference of BODIPY-Schiff dye conformers (kcal/mol) calculated for the ground state with the B3LYP/6-31+G(d,p) method. Purple, red, and green colors correspond to gas, methanol, and DMSO solvents, respectively.
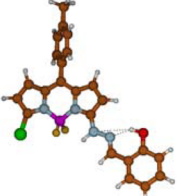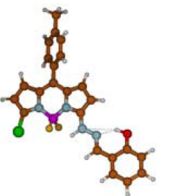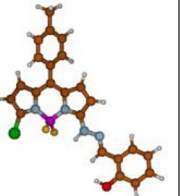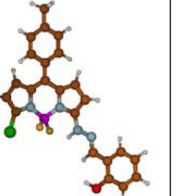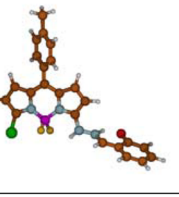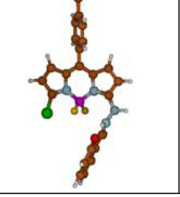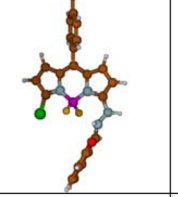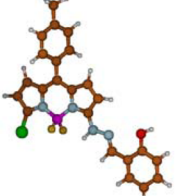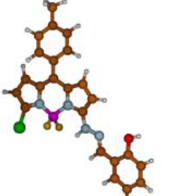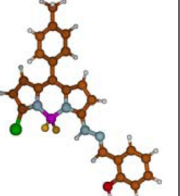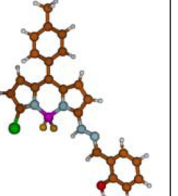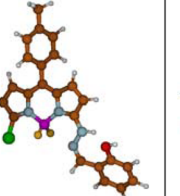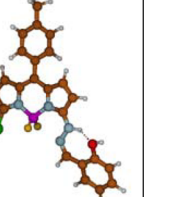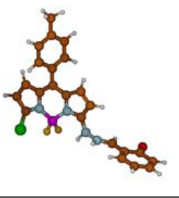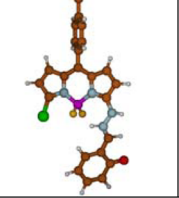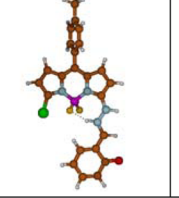
B1		B4			
Ground state	Excited state	Ground state	Excited state	Ground state	Excited state
$\lambda_{abs} = 474.0$	$\lambda_{em} = 551.4$	$\lambda_{abs} = 473.1$	$\lambda_{em} = 541.9$		
B2PT		B3PT			
$\lambda_{abs} = 464.6$	$\lambda_{em} = 491.5$	$\lambda_{abs} = 442.3$	$\lambda_{em} = 477.5$		
B1open		B4open		B5open	
$\lambda_{abs} = 470.0$	$\lambda_{em} = 531.0$	$\lambda_{abs} = 473.5$	$\lambda_{em} = 537.7$	$\lambda_{abs} = 466.6$	$\lambda_{em} = 505.3$
B1PT_N		B3PT_N			
$\lambda_{abs} = 437.4$	$\lambda_{em} = 456.5$	$\lambda_{abs} = 442.3$	$\lambda_{em} = 473.1$		

Figure 6. Conformer's structures of BODIPY-Schiff dye and values of absorption/emission wavelengths calculated with the PBE0/6-31+G(d,p) method.

quantum-mechanical calculations (DFT and TD-DFT; B3LYP/6-31+G(d,p) and PBE0/6-31+G(d,p)) were accomplished for the gas-phase and polar environment (CH$_3$OH and DMSO solvents, PCM approach) (Table S1 of the Supporting

Information). Besides, the calculations were accomplished involving additional solvent molecules (CH_3OH and DMSO) in the gas-phase and the polar environment (CH_3OH and DMSO) considering the PCM model (Figure 6). These calculations substantiate the interpretation of the experimental results and the processes occurring in the molecule.[54−59] Initially the calculations included full optimizations of all possible conformers and tautomers. The optimizations resulted in obtaining 22 conformers (Figures 5, 6, and Figures S3 and S4 of the Supporting Information). Three of four calculated conformers (B1−B3) are characterized by a small deference in energy, $\Delta E_{1−2} = 5.40$ (gas), 5.85 (CH_3OH), and 5.84 (DMSO) kcal/mol and $\Delta E_{1−3} = 8.22$ (gas), 3.80 (CH_3OH), and 3.64 (DMSO) kcal/mol (Figure 5). A similar trend is obtained for both B3LYP and PBE0 methods (cf. Figures 5 and S3 (Supporting Information)). The analysis of the obtained calculations verifies the fact that the growth of the solvent polarity greatly reduces the difference in energy ΔE for conformer B2 (Figure 5 and Table S1 of the Supporting Information). This small difference of energy between the B1−B3 conformers suggests these are present in the different polarity solutions. However, the energy differences between conformers B1 and B5 as well as B1 and B4 are rather significant ($\Delta E_{1−5} = 16.61$ (gas), 14.53 (CH_3OH), and 14.45 (DMSO) kcal/mol); therefore, the probability of the B4 and B5 conformers observation by experimental way is unlikely possible. According to the computed energy, the B1−B3 conformers are more stable than the B5 conformer (Table S1 of the Supporting Information). The stability of the B1 and B2 conformers results from two intramolecular OH···N and NH··· $2x$(F) hydrogen bonds as well as the bifurcated OH···N and OH···F hydrogen bonds for conformer B3. These hydrogen bonds prevail over one weak intramolecular OH···F hydrogen bond in conformer B4 (Figures 6 and S6 (Supporting Information)). This observation is in agreement with the common rule—a hydrogen bonding provokes a decrease of energy of a molecule.[60]

The NH tautomers and open conformers (without intramolecular hydrogen bond, Figure 6) have been calculated. The open isomeric form of the molecule serves as a model featuring the formation of the intermolecular hydrogen bonding under the disruption of the intramolecular hydrogen bonding by means of aprotic polar solvents in experimental condition.

The next stage of the studies is calculations of the absorption band positions in gas and in polar solvents by the TD-DFT and TD-DFT/PCM methods. According to the calculated spectra, the bathochromic shift of the $S_0−S_1$ band with the growing polarity of the solvent (PCM model) is observed for conformers B1−B5, the OH and NH tautomers, and the open conformers (Table 3). It is necessary to note that the calculations of dye molecule with additional solvent molecule did not show a significant change of the absorption band both in the gas phase and the polar environment (PCM approach), Table S2 of the Supporting Information. It is important to stress that the absorption of the NH tautomeric form in the gas phase is conditioned by the $S_0−S_2$ transition because this transition is evoked by the strength of the oscillator ($f = 0.569$) more significantly than the strength of the $S_0−S_1$ transition ($f = 0.108$). The reverse trend, a hypsochromic shift, is traced under the transition from the OH tautomeric form to the NH one (the process of the proton transfer in the intramolecular hydrogen bonding) for each B1−B3 conformers (Table 4). These computational results are supported by experimental

Table 3. Calculated λ_{abs} (B3LYP/6-31+(d,p) and PBE0/6-31+(d,p)) of BODIPY-Schiff Dye in Gas, Methanol, and DMSO

conformer	B3LYP			PBE0
	gas	CH_3OH	DMSO	gas
OH Conformer				
B1	484.7	499.7	504.4	474.0
B2	500.4	511.5	516.4	487.4
B3	502.8	508.5	512.8	490.1
B4	484.0	497.8	501.7	473.1
B5	479.5	492.8	497.1	469.5
NH Conformer				
B1PT	448.9	485.0	486.6	434.1
B2PT	449.3	484.7	486.3	434.1
B3PT	454.6	491.2	490.9	442.3
"Open" OH Conformer				
B1open	479.9	497.4	502.1	470.0
B2open	501.4	504.1	508.7	489.8
B3open	491.4	505.2	509.7	481.1
B4open	483.8	499.4	503.3	473.5
B5open	476.5	491.7	496.3	466.6
"Open" NH Conformer				
B1PT_N	449.3	459.2	461.5	437.4
B2PT_N	449.2	458.8	461.0	436.9
B3PT_N	446.8	459.5	460.5	438.1

Table 4. Changes of Calculated λ_{abs} (B3LYP/6-31+(d,p)) of BODIPY-Schiff Dye upon Transition from OH Tautomeric form to NH Tautomeric Form and "Open" Form

conformer	gas	CH_3OH	DMSO
Transition from OH Tautomeric form to NH tautomeric form			
B1	484.7 → 448.9	499.7 → 485.0	504.4 → 486.6
B2	500.4 → 449.3	511.5 → 484.7	516.4 → 486.3
B3	502.8 → 454.6	508.5 → 491.2	512.8 → 490.9
Transition from OH Tautomeric Form to "Open" OH Form			
B1	484.7 → 479.9	499.7 → 497.4	504.4 → 502.1
B2	500.4 → 501.4	511.5 → 504.1	516.4 → 508.7
B3	502.8 → 491.4	508.5 → 505.2	512.8 → 509.7
B4	484.0 → 483.8	497.8 → 499.4	501.7 → 503.3
B5	479.5 → 476.5	492.8 → 491.7	497.1 → 496.3
Transition from OH Tautomeric Form to "Open" NH Form			
B1	484.7 → 449.3	499.7 → 459.2	504.4 → 461.5
B2	500.4 → 449.2	511.5 → 458.8	516.4 → 461.0
B3	479.5 → 446.8	492.8 → 459.5	497.1 → 460.5

data (cf. spectra for aprotic polar solvent with unipolar solvent, Figures 1 and S1 (Supporting Information)). Moreover, the transition from OH tautomeric form to the open OH form (a model of the disruption of intramolecular hydrogen bonding and the formation of the intermolecular hydrogen bonding) also evokes a hypsochromic shift (Table 4). These computational results make it possible to properly interpret the experimental data (compare spectra in Figures 1 and S1 (Supporting Information)). It is necessary to note that the absorption band also shifts hypsochromically under the transition from OH tautomeric form to open NH conformer, whereas the change of polarity (gas → methanol → DMSO) for open NH conformer brings about the bathochromic shift (Table 3).

Summarizing the data for the absorption transitions obtained by the calculations, one can conclude that the transformation

from the most stable conformer (OH conformer) to the less stable conformers (open form and NH tautomer) should lead to the hypsochromic shift of the absorption band. However, the polarity increase (PCM model) of the solvent should result in the bathochromic shift for each of the conformers. Importantly, the first phenomenon (the change of conformation) conditions the more significant shift than the second one (the influence of solvent polarity). According to the aforesaid discussion, the processes of the proton transfer, the disruption of intramolecular hydrogen bond, and the process of isomerization must evoke the hypsochromic shift of the S_0-S_1 absorption band for the studied BODIPY-Schiff dye. This conclusion based on the calculation results is in agreement with the experimental one (Figure 4). It is necessary to note that a similar phenomenon (the increase of the solvent polarity brought about the batochromic shift of the $\pi-\pi^*$ band, whereas the disruption of intramolecular hydrogen bonding and the formation of the intermolecular hydrogen bonding and the hypsochromic shift) is observed for o-hydroxy benzamides by experimental method.[61]

Full optimization of the molecule in the excited state results mostly in other conformers. In terms of the calculations for the excited state, they are rather hard to complete. A good example is the NH tautomer calculation by B3LYP method; under optimization this form inevitably takes the OH tautomeric form. Therefore, additional calculations were accomplished by the PBE0 method. As to the calculated emission band, for the gas phase it lays in the region of 550 nm (Figure 6 and Table S2 of the Supporting Information). This result obtained by B3LYP (552.9 nm) and PBE0 (551.4 nm) methods properly correlates with the experimental data obtained in nonpolar solvents (Table 1).

The calculations carried out by B3LYP method considering the PCM model and additional solvent molecules (Table S2 of the Supporting Information) show that the environmental polarity (transition from the gas phase to either CH_3OH and DMSO) greatly shifts the emission band bathochromically. This trend taken by TD-DFT calculations is in agreement with the experimental one. Transition from methanol (546 nm) to DMSO (627 nm) provokes the shift to 63 nm. However, the value of the shift obtained by the calculations is significantly larger and equals 204.8 nm. The obtained results (a great difference between the experimental and computational values) are also shown in works by Jacquemin et al.[54−58] It is important to underline that the observed trends obtained by the experimental and computational methods are in accordance. This conclusion also coincides with the conclusions drawn by ref 57.

CONCLUSION

This work presents the synthesis combining of two fragments of o-hydroxy aryl Schiff base and BODIPY chromophore. The obtained substance has been studied in both the ground and excited states by experimental and computational methods. The dependencies obtained experimentally point out the presence of two processes, under the transition from the ground and excited one or the excited state. According to the quantum-mechanical calculations these processes are likely to be the processes of isomerization and the proton transfer.

ASSOCIATED CONTENT

Ⓢ Supporting Information

Tables listing calculated photophysical data, calculated λ_{abs} and λ_{em} values of BODIPY-Schiff dye in different solvents, and calculated structures and λ_{ab} and λ_{em} parameters of BODIPY-Schiff dye in respective ground and excited states, figures showing absorption and emission spectra of BODIPY-Schiff dye in different solvents, ground and excited state energy differences of the conformers, a reaction scheme, and NMR spectra, and text describing experimental procedures and results. This material is available free of charge via the Internet at http://pubs.acs.org.

AUTHOR INFORMATION

Corresponding Author

*E-mail: aleksander.filarowski@chem.uni.wroc.pl.

Notes

The authors declare no competing financial interest.

REFERENCES

(1) de Silva, A. P.; Gunaratne, H. Q. N.; McCoy, C. P. A Molecular Photoionic AND Gate Based on Fluorescent Signalling. *Nature* **1993**, *364*, 42−44.

(2) Brouwer, A. M.; Frochot, C.; Gatti, F. G.; Leigh, D. A.; Mottier, L.; Paolucci, F.; Roffia, S.; Wurpel, G. W. H. Photoinduction of Fast, Reversible Translational Motion in a Hydrogen-Bonded Molecular Shuttle. *Science* **2001**, *291*, 2124−2128.

(3) Andréasson, J.; Pischel, U. Smart Molecules at Work—Mimicking Advanced Logic Operations. *Chem. Soc. Rev.* **2010**, *39*, 174−188.

(4) Loudet, A.; Burgess, K. BODIPY Dyes and Their Derivatives: Syntheses and Spectroscopic Properties. *Chem. Rev.* **2007**, *107*, 4891−4932.

(5) Ziessel, R.; Ulrich, G.; Harriman, A. The Chemistry of BODIPY: A New El Dorado for Fluorescence Tools. *New J. Chem.* **2007**, *31*, 7838−7851.

(6) Kobayashi, H.; Ogawa, M.; Alford, R.; Choyke, P. L.; Urano, Y. New Strategies for Fluorescent Probe Design in Medical Diagnostic Imaging. *Chem. Rev.* **2010**, *110*, 2620−2640.

(7) Boens, N.; Leen, V.; Dehaen, W. Fluorescent Indicators Based on BODIPY. *Chem. Soc. Rev.* **2012**, *41*, 1130−1172.

(8) Rurack, K.; Kollamannsberg, M.; Daub, J. A Highly Efficient Sensor Molecule Emitting in the Near Infra-red (NIR): 3,5-Distyryl-Substituted Difluoroboradiaza-s-indacene. *New J. Chem.* **2001**, *25*, 289−292.

(9) Benstead, M.; Mehl, G. H.; Boyle, R. W. 4,4′-Difluoro-4-bora-3a,4a-diaza-s-indacenes (BODIPYs) as Components of Novel Light Active Materials. *Tetrahedron* **2011**, *67*, 3573−3601.

(10) Hadjoudis, E.; Mavridis, I. Photochromism and Thermochromism of Schiff Bases in the Solid State: Structural Aspects. *Chem. Soc. Rev.* **2004**, *33*, 579−588.

(11) Antonov, L., Ed. *Tautomerism: Methods and Theories*; Wiley-VCH: Weinheim, Germany, 2014.

(12) Nedeltcheva, D.; Antonov, L. Relative strength of the intramolecular hydrogen bonding in 1-phenylazo-naphthalen-2-ol and 1-phenyliminomethyl-naphtahlen-2-ol. *J. Phys. Org. Chem.* **2009**, *22*, 274−281.

(13) Zgierski, J.; Grabowska, A. Theoretical Approach to Photochromism of Aromatic Schiff Bases: A Minimal Chromophore Salicylidene Methylamine. *J. Chem. Phys.* **2000**, *113*, 7845−7852.

(14) Sliwa, M.; Mouton, N.; Ruckebusch, C.; Poisson, L.; Idrissi, A.; Aloise, S.; Potier, L.; Dubois, J.; Poizat, O.; Buntinx, G. Investigation of Ultrafast Photoinduced Processes for Salicylidene Aniline in Solution and Gas Phase: Toward a General Photo-dynamical Scheme. *Photochem. Photobiol. Sci.* **2010**, *9*, 661−669.

(15) Ziółek, M.; Gil, M.; Organero, J. A.; Douhal, A. What Is the Difference Between the Dynamics of Anion- and Keto-type of Photochromic Salicylaldehyde Azine. *Phys. Chem. Chem. Phys.* **2010**, *12*, 2107−2115.

(16) Ulrich, G.; Nastasi, F.; Retailleau, P.; Puntoriero, F.; Ziessel, R.; Campagna, S. Luminescent Excited-State Intramolecular Proton-Transfer (ESIPT) Dyes Based on 4-Alkyne-Functionalized [2,2′-Bipyridine]-3,3′-diol Dyes. *Chem.—Eur. J.* **2008**, *14*, 4381−4392.

(17) Jakobsen, J. J.; Stork, J. R.; Magde, D.; Cohen, S. M. Hydrogen-Bond Rigidified BODIPY Dyes. *Dalton Trans.* **2010**, *39*, 957−962.

(18) Xiao, S.; Zou, Y.; Wu, J.; Zhou, Y.; Yi, T.; Li, F.; Huang, C. Hydrogen Bonding Assisted Switchable Fluorescence in Self-Assembled Complexes Containing Diarylethene: Controllable Fluorescent Emission in the Solid State. *J. Mater. Chem.* **2007**, *17*, 2483−2489.

(19) Olivier, J.-H.; Haefele, A.; Retailleau, P.; Ziessel, R. Borondipyrromethene Dyes with Pentane-2,4-dione Anchors. *Org. Lett.* **2010**, *12*, 408−411.

(20) Waluk, J. Conformational Aspects of Intra- and Intermolecular Exited State Proton Transfer. In *Conformational Analysis of Molecules in Excited State*; Waluk, J., Ed.; Wiley-VCH: New York, 2000; pp 57−111.

(21) Borowicz, P.; Grabowska, A.; Les, A.; Kaczmarek, L.; Zagrodzki, B. New Phototautomerizing Systems: Non-Symmetric Derivatives of [2,2′-Bipyridyl]-3,3′-diol. *Chem. Phys. Lett.* **1998**, *291*, 351−359.

(22) Weller, A. Uber die Fluoreszenz der Salizylsaure und Verwandter Verbindungen. *Naturwissenschaften* **1955**, *42*, 175−176.

(23) Alamiry, M. A. H.; Harriman, A.; Mallon, L. J.; Ulrich, G.; Ziessel, R. Energy- and Charge-Transfer Processes in a Perylene−BODIPY−Pyridine Tripartite Array. *Eur. J. Chem.* **2008**, 2774−2782.

(24) Yang, P.; Zhao, J.; Wu, W.; Yu, X.; Liu, Y. Accessing the Long-Lived Triplet Excited States in Bodipy-Conjugated 2-(2-Hydroxyphenyl) Benzothiazole/Benzoxazoles and Applications as Organic Triplet Photosensitizers for Photooxidations. *J. Org. Chem.* **2012**, *77*, 6166−6178.

(25) Shiraishi, Y.; Maehara, H.; Sugii, T.; Wang, D.; Hirai, T. A BODIPY-Indole Conjugate as a Colorimetric and Fluorometric Probe for Fluoride Anion Detection. *Tetrahedron Lett.* **2009**, *50*, 4293−4296.

(26) Baruah, M.; Qin, W.; Flors, C.; Hofkens, J.; Vallee, R. A. L.; Beljonne, D.; Van der Auweraer, M.; De Borggraeve, W. M.; Boens, N. Solvent and pH Dependent Fluorescent Properties of a Dimethylaminostyryl Borondipyrromethene Dye in Solution. *J. Phys. Chem. A* **2006**, *110*, 5998−6009.

(27) Dąbrowski, J.; Kamieńska-Trela, K. Electronic Spectra of alpha, beta-Unsaturated Carbonyl Compounds. I. An Evaluation of Increments Characteristic of Changes in Configuration (cis/trans) and Conformation (s-cis/s-trans) Based on Direct Observation of the Isomerization of Enamino Aldehydes and Ketones. *J. Am. Chem. Soc.* **1976**, *98*, 2826−2834.

(28) Qin, W.; Baruah, M.; Sliwa, M.; Van der Auweraer, M.; De Borggraeve, W. M.; Beljonne, D.; Van Averbeke, B.; Boens, N. Ratiometric, Fluorescent BODIPY Dye with Aza Crown Ether Functionality: Synthesis, Solvatochromism, and Metal Ion Complex Formation. *J. Phys. Chem. A* **2008**, *112*, 6104−6114.

(29) Rurack, K.; Kollmannsberger, M.; Daub, J. Molecular Switching in the Near Infrared (NIR) with a Functionalized Boron−Dipyrromethene Dye. *Angew. Chem., Int. Ed.* **2001**, *40*, 385−387.

(30) Galangau, O.; Dumas-Verdes, C.; Meallet-Renault, R.; Clavier, G. Rational Design of Visible and NIR Distyryl-BODIPY Dyes from a Novel Fluorinated Platform. *Org. Biomol. Chem.* **2010**, *8*, 4546−4553.

(31) Murtagh, J.; Frimannsson, D. O.; O'Shea, D. F. Azide Conjugatable and pH Responsive Near-Infrared Fluorescent Imaging Probes. *Org. Lett.* **2009**, *11*, 5386−5389.

(32) Rohand, T.; Baruah, M.; Qin, W. W.; Boens, N.; Dehaen, W. Functionalisation of Fluorescent BODIPY Dyes by Nucleophilic Substitution. *Chem. Commun. (Cambridge, U. K.)* **2006**, 266−268.

(33) Dilek, O.; Bane, S. L. Synthesis and Spectroscopic Characterization of Fluorescent Boron Dipyrromethene-Derived Hydrazones. *J. Fluoresc.* **2011**, *21*, 347−354.

(34) Olmsted, J. Calorimetric Determinations of Absolute Fluorescence Quantum Yields. *J. Phys. Chem.* **1979**, *83*, 2581−2584.

(35) Boens, N.; Qin, W.; Basarić, N.; Hofkens, J.; Ameloot, M.; Pouget, J.; Lefèvre, J.-P.; Valeur, B.; Gratton, E.; van de Ven, M.; Silva.; et al. Fluorescence Lifetime Standards for Time and Frequency Domain Fluorescence Spectroscopy. *Anal. Chem.* **2007**, *79*, 2137−2149.

(36) Crovetto, L.; Orte, A.; Talavera, E. M.; Alvarez-Pez, J. M.; Cotlet, M.; Thielemans, J.; De Schryver, F. C.; Boens, N. Global Compartmental Analysis of the Excited-State Reaction between Fluorescein and (±)-N-Acetyl Aspartic Acid. *J. Phys. Chem. B* **2004**, *108*, 6082−6092.

(37) Frisch, M. J.; Trucks, G. W.; Schlegel, H. B.; Scuseria, G. E.; Robb, M. A.; Cheeseman, J. R.; Montgomery, J. A., Jr.; Vreven, T.; Kudin, K. N.; Burant, J. C.; et al. *Gaussian 03*, revision B.03; Gaussian: Wallingford, CT, USA, 2004.

(38) McLean, A. D.; Chandler, G. S. Contracted Gaussian Basis Sets for Molecular Calculations. I. Second Row Atoms, Z=11−18. *J. Chem. Phys.* **1980**, *72*, 5639−5648.

(39) Krishnan, R.; Binkley, J. S.; Seeger, R.; Pople, J. A. Self-Consistent Molecular Orbital Methods. XX. A Basis Set for Correlated Wave Functions. *J. Chem. Phys.* **1980**, *72*, 650−654.

(40) Clark, T.; Chandrasekhar, J.; Spitznagel, G. W.; Schleyer, P. v. R. Efficient Diffuse Function-Augmented Basis Sets for Anion Calculations. III. The 3-21+G Set for First-Row Elements, Li-F. *J. Comput. Chem.* **1983**, *4*, 294−301.

(41) Becke, A. D. A New Mixing of Hartree-Fock and Local Density-Functional Theories. *J. Chem. Phys.* **1993**, *98*, 1372−1377.

(42) Lee, C.; Yang, W.; Parr, R. G. Development of the Colle−Salvetti Correlation-Energy Formula into a Functional of the Electron Density. *Phys. Rev. B: Condens. Matter Mater. Phys.* **1988**, 785−789.

(43) Perdew, J. P.; Burke, K.; Ernzerhof, M. Generalized Gradient Approximation Made Simple. *Phys. Rev. Lett.* **1996**, *77*, 3865−3868.

(44) Adamo, C.; Barone, V. Toward Reliable Density Functional Methods without Adjustable Parameters: The PBE0 Method. *J. Chem. Phys.* **1999**, *110*, 6158−6170.

(45) Scheiner, S. *Hydrogen Bonding: A Theoretical Perspective*; Oxford University Press: New York, 1997.

(46) Hohenberg, P.; Kohn, W. Inhomogeneous Electron Gas. *Phys. Rev.* **1964**, *136*, B864−B871.

(47) Bauernschmitt, R.; Ahlrichs, R. Treatment of Electronic Excitations within the Adiabatic Approximation of Time Dependent Density Functional Theory. *Chem. Phys. Lett.* **1996**, *256*, 454−464.

(48) Casida, M. E.; Jamorski, C.; Casida, K. C.; Salahud, D. R. Molecular Excitation Energies to High-Lying Bound States from Time-Dependent Density-Functional Response Theory: Characterization and Correction of the Time-Dependent Local Density Approximation Ionization Threshold. *J. Chem. Phys.* **1998**, *108*, 4439−4449.

(49) Tomasi, J.; Mennucci, B.; Cammi, R. Quantum Mechanical Continuum Solvation Models. *Chem. Soc. Rev.* **2005**, *105*, 2999−3094.

(50) Hattig, C.; Jorgensen, P. Polarizabilities of CO, N$_2$, HF, Ne, BH, and CH$^+$ from *ab initio* calculations: Systematic studies of electron correlation, basis set errors, and vibrational contributions. *J. Chem. Phys.* **1998**, *109*, No. 4745.

(51) Filarowski, A.; Kluba, M.; Cieslik-Boczula, K.; Kochel, A.; Pandey, L.; De Borggraeve, W. M.; Van der Auweraer, M.; Catalan, J.; Boens, N. Generalized Solvent Scales as a Tool for Investigating Solvent Dependence of Spectroscopic and Kinetic Parameters. Application to Fluorescent BODIPY Dyes. *Photochem. Photobiol. Sci.* **2010**, *9*, 996−1008.

(52) Boens, N.; Qin, W.; Baruah, M.; De Borggraeve, W. M.; Filarowski, A.; Smisdom, N.; Ameloot, M.; Crovetto, L.; Talavera, E. M.; Alvarez-Pez, J. M. Rational Design, Synthesis and Spectroscopic and Photophysical Properties of a Visible-Light-Excitable, Ratiometric, Fluorescent Near-Neutral pH Indicator Based on BODIPY. *Chem.— Eur. J.* **2011**, *17*, 10924−10934.

(53) Deniz, E.; Isbasar, G. C.; Bozdemir, O. A.; Yildirim, L. T.; Siemiarczuk, A. A.; Akkaya, E. U. Bidirectional Switching of Near IR Emitting Boradiazaindacene Fluorophores. *Org. Lett.* **2008**, *10*, 3401− 3403.

(54) Jacquemin, D.; Planchat, A.; Adamo, C.; Mennucci, B. TD-DFT Assessment of Functionals for Optical 0−0 Transitions in Solvated Dyes. *J. Chem. Theory Comput.* **2012**, *8*, 2359−2372.

(55) Chibani, S.; Le Guennic, B.; Charaf-Eddin, A.; Laurent, A. D.; Jacquemin, D. Revisiting the Optical Signatures of BODIPY with ab Initio Tools. *Chem. Sci.* **2013**, *4*, 1950−1963.

(56) Laurent, A. D.; Jacquemin, D. TD-DFT Benchmarks: A Review. *Int. J. Quantum Chem.* **2013**, *113*, 2019−2039.

(57) Laurent, A. D.; Adamo, C.; Jacquemin, D. Dye Chemistry with Time-Dependent Density Functional Theory. *Phys. Chem. Chem. Phys.* **2014**, *16*, 14334−14356.

(58) Charaf-Eddin, A.; Le Guennic, B.; Jacquemin, D. Optical Signatures of Borico Dyes: A TD-DFT Analysis. *Theor. Chem. Acc.* **2014**, *133*, No. 1456.

(59) Prieto, J. B.; Arbeloa, F. L.; Martinez, V. M.; Arbeloa, L. Theoretical study of the ground and excited electronic states of pyrromethene 546 laser dye and related compounds. *Chem. Phys.* **2004**, *296*, 13−22.

(60) Hadži, D. *Theoretical Treatments of Hydrogen Bonding*; John Wiley & Sons: Chichester, New York, Weinheim, Brisbane, Singapore, Toronto, 1997.

(61) Majewska, P.; Pajak, A.; Rospenk, M.; Filarowski, A. Intra- Versus Intermolecular Hydrogen Bonding Equilibrium in 2-hydroxy-N,N-diethylbenzamide. *J. Phys. Org. Chem.* **2009**, *22*, 130−137.